Lyapunov instability of fluids composed of rigid diatomic molecules

István Borzsák

Laboratory of Theoretical Chemistry, Eötvös University, P.O. Box 32, H-1518 Budapest 112, Hungary

H. A. Posch

Institut für Experimentalphysik, Universität Wien, Boltzmanngasse 5, A-1090 Wien, Austria

András Baranyai

Laboratory of Theoretical Chemistry, Eötvös University, P.O. Box 32, H-1518 Budapest 112, Hungary

We study the Lyapunov instability of a two-dimensional fluid composed of rigid diatomic molecules, with two interaction sites each, and interacting with a Weeks-Chandler-Anderson site-site potential. We compute full spectra of Lyapunov exponents for such a molecular system. These exponents characterize the rate at which neighboring trajectories diverge or converge exponentially in phase space. Qualitative different degrees of freedom, such as rotation and translation, affect the Lyapunov spectrum differently. We study this phenomenon by systematically varying the molecular shape and the density. We define and evaluate "rotation numbers" measuring the time averaged modulus of the angular velocities for vectors connecting perturbed satellite trajectories with an unperturbed reference trajectory in phase space. For reasons of comparison, various time correlation functions for translation and rotation are computed. The relative dynamics of perturbed trajectories is also studied in certain subspaces of the phase space associated with center-of-mass and orientational molecular motion.

PACS number(s): 61.25.Em, 05.45.+b, 02.70.Ns, 05.20.−y

I. INTRODUCTION

The chaotic molecular motion in fluids and (nonlinear) solids has been studied in the past mainly in terms of correlation functions or related power spectra of assorted dynamical variables. There is, however, a more fundamental point of view: The basic underlying dynamical processes are collisions (interactions) between particles with convex potential surfaces. As a consequence, the phase-space trajectory is highly unstable, which is reflected in a very sensitive dependence on initial conditions. This phenomenon is characterized in terms of the set of Lyapunov exponents $\{\lambda_l\}, l=1,\dots,L$, usually ordered from the largest to the smallest. The largest exponent λ_1 describes the time-averaged logarithmic rate at which nearby phase-space trajectories separate. The sums of exponents $\Sigma_{i=1}^{l}\lambda_i$ describe the expansion or contraction rates of l-dimensional phase-space objects. Thus the Lyapunov exponents represent the time-averaged local deformation rates in the neighborhood of a phase-space trajectory specified by the time evolution of specially selected perturbation vectors $\delta_l(t)$. From a practical point of view the precise orientation of the set of initial vectors $\{\delta_l(0)\}$ is not known, nor is it needed for the determination of the λ_l. This is discussed in more detail in Sec. II. The total number L of exponents is equal to the dimensionality of the phase space and the whole set of exponents is referred to as the Lyapunov spectrum. For the evaluation of all L exponents the simultaneous integration of $L(L+1)$ first-order differential equations is required. The method has therefore been restricted to rather low-dimensional dynamical systems in the past. The feasibility of such studies for many-body systems has been demonstrated by Posch and

Hoover [1,2] who investigated fluid systems with up to 100 atoms in two dimensions.

Lyapunov spectra of Hamiltonian systems in thermal equilibrium exhibit a pronounced symmetry, which helps to reduce the number of differential equations to $L(L+2)/2$: for each positive exponent there exists another negative exponent with equal absolute magnitude. This is referred to as Smale pairing [1] or conjugate pairing [3,4]. It is a consequence of the symplectic nature of the equations of motion [5], which means that the phase flow, viewed as a canonical transformation of the phase space onto itself, leaves the differential two-form $\Sigma_{i=1}^{L/2} dp_i \wedge dq_i$ invariant. Here the sum is over all degrees of freedom and p_i and q_i denote all components of particle momenta and positions, respectively. Due to this pairing symmetry the calculation may be restricted to the positive exponents, thus permitting the simulation of more complex and larger systems. With the available computer hardware systems with up to 400 degrees of freedom may be simulated at present [6] by far exceeding the complexity one usually encounters when studying dynamical systems with a low-dimensional phase space [7].

For atomic fluids one finds that the shape of the Lyapunov spectrum changes qualitatively if the density is isothermally increased from that of a dense gas to solid densities [8] and that the largest Lyapunov exponent λ_1 exhibits a maximum at the solid-fluid phase transition density [8,9]. From a simulation of thermostated butane molecules one may further deduce that the largest contribution to λ_1, and therefore the largest source for chaos, is due to the torsional motion around the central CC bond. The other degrees of freedom contribute mainly to the smaller exponents [10]. This conclusion has been reached by observing the variations in the Lyapunov spectrum of a Nosé-Hoover-thermostated mol-

ecule, if various contributions to the molecular Hamiltonian specifying different degrees of freedom are selectively switched off. Considering these examples, we may expect that also for molecular fluids the stretching and contraction properties are very differently affected by translation and rotation and that, as a consequence, the shape of the Lyapunov spectra will strongly depend on the state of the system. To clarify this point we report in this paper results of a molecular dynamics simulation study of a simple planar molecular fluid in equilibrium consisting of N rigid homonuclear diatomic molecules with anisotropy d/σ. Here d is the fixed bond length separating the two interaction sites of a molecule, and σ is an atomic-size parameter. d, or the related moment of inertia, and the molecular number density n^* are two independent parameters with which the emphasis may be conveniently shifted between translational and rotational dynamics, at the same time varying the respective relaxation times. We measure the associated changes in the (in)stability properties of the phase-space trajectories.

In Sec. II we define our model fluid and indicate our method of simulating the reference trajectory. In Sec. III we briefly outline the methods for the evaluation of Lyapunov spectra. We define so-called rotation spectra for the vectors δ_l connecting neighboring trajectories in phase space [8]. It turns out that it is useful to study also the projected motion of these vectors in subspaces of the phase space such as the respective configurational and momentum spaces for translational and rotational motion. To make contact with the more traditional analysis of molecular dynamics in fluids, we also evaluate correlation functions pertinent for these degrees of freedom. In Sec. IV we summarize our results. They are discussed further in Sec. V, where we speculate also about possible interpretations of the Lyapunov spectra in terms of suitably defined collective modes in dense fluids.

II. MODEL FLUID

Simulations were performed for a purely classical system consisting of $N = 18$ rigid homonuclear diatomic molecules in a two-dimensional square box of area (volume) V and with periodic boundary conditions. The two interaction sites of each molecule are separated by a rigid distance d along the molecular axis and sites on different molecules separated by r interact with a purely repulsive Weeks-Chandler-Anderson potential

$$\phi(r) = \begin{cases} 4\epsilon[(\sigma/r)^{12} - (\sigma/r)^6] + \epsilon, & r < 2^{1/6}\sigma \\ 0, & r \geq 2^{1/6}\sigma. \end{cases} \quad (1)$$

The total intermolecular potential energy Φ is taken to be pairwise additive. Reduced units are used throughout, for which ϵ, σ, and the atomic mass m are unity. The equations of motion for the $2N$ interaction sites were augmented with constraint forces keeping the bond length d for each molecule fixed [11]:

$$\dot{\mathbf{q}}_\alpha = \mathbf{p}_\alpha/m,$$

$$\dot{\mathbf{p}}_1 = \mathbf{f}_1 + \mu(\mathbf{q}_2 - \mathbf{q}_1), \quad (2)$$

$$\dot{\mathbf{p}}_2 = \mathbf{f}_2 - \mu(\mathbf{q}_2 - \mathbf{q}_1).$$

Here $\mathbf{q}_\alpha, \mathbf{p}_\alpha$ are the respective position and momentum vectors of the two interaction sites of a molecule, $\alpha = 1,2$, and $\mathbf{f}_\alpha = -\nabla_\alpha \Phi$ is the force on site α. Furthermore,

$$\mu = \frac{(\mathbf{p}_2 - \mathbf{p}_1)^2/m + (\mathbf{q}_2 - \mathbf{q}_1)\cdot(\mathbf{f}_2 - \mathbf{f}_1)}{2(\mathbf{q}_2 - \mathbf{q}_1)^2} \quad (3)$$

is the Lagrange multiplier for the holonomic constraint $(\mathbf{q}_2 - \mathbf{q}_1)^2 - d^2 = 0$ for this molecule. The initial conditions were chosen such that the total center-of-mass velocity was zero.

For the evaluation of the Lyapunov exponents and the ensuing discussion it is useful to represent the state of the system by the $6N$-dimensional state vector $\Gamma(t) = \{x_i, y_i, \dot{x}_i, \dot{y}_i, \eta_i, \dot{\eta}_i\}$, $i = 1, N$, where x_i, y_i and $\dot{x}_i, \dot{y}_i$ are the center of mass coordinates and momenta, respectively, of molecule i, and η_i is the angle the molecular axis of i makes with some arbitrary direction. $\dot{\eta}_i$ is the corresponding angular velocity. For each molecule i these quantities may be easily computed from the instantaneous positions and momenta of the interaction sites.

III. LYAPUNOV EXPONENTS AND ROTATION NUMBERS

The equation of motion for the state vector $\Gamma(t)$ is conveniently written as an autonomous system of first-order differential equations

$$\dot{\Gamma}(t) = \mathbf{G}(\Gamma(t)). \quad (4)$$

Its solution defines a flow $\Gamma(t) = \Phi_t(\Gamma(0))$ in phase space. Let $\Gamma(0)$ be the initial condition of a reference trajectory, $\Gamma_s(0)$ the initial point of a neighboring perturbed trajectory, and let these two points be connected by a parametrized path $C_0(s)$ with a perturbation parameter s such that $\lim_{s \to 0} \Gamma_s(0) = \Gamma(0)$. At time t these points will be mapped by the flow onto the points $\Gamma(t) = \Phi_t(\Gamma(0))$ and $\Gamma_s(t) = \Phi_t(\Gamma_s(0))$ and the path $C_0(s)$ into $C_t(s)$. Now we can define a finite-length tangent vector at $t = 0$,

$$\delta(0) = \lim_{s \to 0} \frac{\Gamma_s(0) - \Gamma(0)}{s}, \quad (5)$$

associated with an initial perturbation $\Gamma_s(0) - \Gamma(0)$ of the reference trajectory in phase space. As time goes on, this perturbation develops into $\Gamma_s(t) - \Gamma(t)$ and the associated tangent vector becomes

$$\delta(t) = \lim_{s \to 0} \frac{\Gamma_s(t) - \Gamma(t)}{s}. \quad (6)$$

The change of the length of this vector during the time interval t determines the stability of the reference trajectory due to the initial infinitesimal perturbation. $\delta(t)$ may be viewed as a vector comoving and corotating with the phase flow in the immediate neighborhood of the phase point. It specifies a direction in phase space that varies with time. The equations of motion for $\delta(t)$ are obtained by linearizing the original motion equations (4),

$$\dot{\delta}(t) = \mathbf{D}(\Gamma(t))\cdot\delta(t), \quad (7)$$

where $\mathbf{D}(\Gamma) \equiv [(\partial/\partial\Gamma)\mathbf{G}(\Gamma)]$ is an $L \times L$ matrix and is referred to as the stability matrix. The formal solution of (7) may be written as

$$\boldsymbol{\delta}(t) = \mathbf{M}(t; \boldsymbol{\delta}(0)) \cdot \boldsymbol{\delta}(0), \tag{8}$$

where the operator $\mathbf{M}$ is a time ordered exponential of $\int \mathbf{D}((\Gamma(t'))dt'$. According to the multiplicative ergodic theorem by Oseledec [13,14] the Lyapunov exponents

$$\lambda_l = \lim_{t \to \infty} \frac{1}{t} \ln |\mathbf{M}(t; \boldsymbol{\delta}(0))\mathbf{u}_l|$$

$$= \lim_{t \to \infty} \frac{1}{2t} \ln |\mathbf{u}_l^\dagger \cdot \mathbf{H}(t; \boldsymbol{\delta}(0)) \cdot \mathbf{u}_l| \tag{9}$$

exist for mixing systems and are independent of the initial conditions. In this equation $\mathbf{u}_l$ denote the L orthonormal eigenvectors of the real and symmetric matrix $\mathbf{H}(t; \boldsymbol{\delta}(0)) = \mathbf{M}(t; \boldsymbol{\delta}(0))^\dagger \mathbf{M}(t; \boldsymbol{\delta}(0))$, where a dagger means transpose. They may be taken as the basis for an arbitrary inital vector $\boldsymbol{\delta}(0)$, for which the long-time behavior is ultimately determined by that vector component $\boldsymbol{\delta}(0) \cdot \mathbf{u}_l$ with the largest associated Lyapunov exponent.

The classical algorithm for the calculation of the complete spectrum of Lyapunov exponents due to Benettin et al. [15,16]. and others [17,18,14] requires the simultaneous integration of the original reference system (4) and of L sets of the linearized equations (7) for L initial tangent vectors $\boldsymbol{\delta}_l(0)$ taken to be orthonormal. However, due to the stretching and folding operations of the phase flow, these vectors will not stay orthonormal for $t > 0$ but will be stretched and rotated into the direction of the largest phase-space expansion corresponding to the largest exponent and eventually diverge. This is prevented by reorthonormalizing the vectors after every few time steps. The Lyapunov exponents are determined from the time-averaged contraction or expansion factors for the vector norms.

A conceptual refinement of this algorithm has been proposed by Hoover et al. [12,1] and independently by Goldhirsch et al. [19].. It has again been reinvented since then [20]. In this method the vectors $\boldsymbol{\delta}_l$ are constrained to remain orthonormal for all times $t > 0$ by the introduction of constraining forces added to the right-hand side of the linearized motion equations:

$$\dot{\boldsymbol{\delta}}_l(t) = \mathbf{D}(\Gamma(t))\boldsymbol{\delta}_l - \sum_{l'=1}^{l} \lambda_{l'l} \boldsymbol{\delta}_{l'}. \tag{10}$$

The $\lambda_{l',l}$ are time-dependent Lagrange multipliers and are determined from the orthonormality conditions $(\boldsymbol{\delta}_l \cdot \boldsymbol{\delta}_{l'}) = \delta_{ll'}$:

$$\lambda_{l'l} = \begin{cases} \boldsymbol{\delta}_l^\dagger \cdot \mathbf{D} \cdot \boldsymbol{\delta}_l & \text{if } l' = l \\ \boldsymbol{\delta}_l^\dagger \cdot \mathbf{D} \cdot \boldsymbol{\delta}_{l'} + \boldsymbol{\delta}_{l'}^\dagger \cdot \mathbf{D} \cdot \boldsymbol{\delta}_l & \text{if } l' < l. \end{cases} \tag{11}$$

The Lyapunov exponents are given by the time-averaged diagonal multipliers

$$\lambda_l = \langle \lambda_{ll}(t) \rangle. \tag{12}$$

This algorithm is equivalent to the classical algorithm with continuous reorthonormalization and yields solutions for the tangent vectors $\boldsymbol{\delta}_l(t)$ identical to the classical ones, if in the latter case the vectors are reorthonormalized after every time step. However, the Eqs. (11), together with (arbitrary) initial conditions may be considered as the defining equations for the orthonormal vectors $\boldsymbol{\delta}_l(t)$. They emphasize another property of tangent-space dynamics that has been virtually ignored up to now [19,8], namely, the rotation of the orthonormal tangent vectors.

We have seen that the solution of Eqs. (11) constitutes an orthonormal set of vectors that continuously change their orientation in tangent space with instantaneous angular velocities $\Delta\Theta_l(t)/\Delta t$. The vectors are forced to remain orthogonal to each other through the force terms proportional to the off-diagonal Lagrange multipliers in Eq. (9). If viewed in phase space, these orthonormal vectors move with the state point along the reference trajectory and simultaneously reorient such that $\boldsymbol{\delta}_1$ always turns toward the direction of fastest phase-space expansion, $\boldsymbol{\delta}_2$ into a perpendicular direction with the second largest growth, and so forth. As a measure for this unitary rotation we have computed an averaged angular velocity for each vector $\boldsymbol{\delta}_l$ defined by

$$\omega_l = \frac{1}{N_t} \sum_{n=1}^{N_t} \frac{\cos^{-1}[\boldsymbol{\delta}_l(t_n) \cdot \boldsymbol{\delta}_l(t_n + \Delta t)]}{\Delta t}$$

$$= \frac{1}{N_t} \sum_{n=1}^{N_t} \frac{|\Delta\Theta_l(t_n)|}{\Delta t}, \tag{13}$$

where $\Delta\Theta_l(t_n)$ is the angle by which the unit vector $\boldsymbol{\delta}_l$ reorients during a time step Δt at time $t_n = n\Delta t$ and N_t is the number of time steps of the simulation. We refer to these numbers as "rotation numbers" and to their whole set as the "rotation spectrum" [8]. Thus ω_l is the time-averaged modulus of the angular velocity for the reorienting vector $\boldsymbol{\delta}_l(t)$ in phase space.

We stress that, unlike the Lyapunov exponents, the rotation numbers defined in (13) depend on the metric of the phase space and of the coordinate system used. There is no multiplicative ergodic theorem for these quantities, although they are independent of the choice of the initial conditions. In this respect they are on the same level of theoretical significance as the instantaneous finite-time Lyapunov exponents, which also depend on the choice of the coordinate system [7]. This issue clearly needs further investigation. In spite of these theoretical restrictions, the rotation numbers still convey important information about the phase-space dynamics. For example, for isothermal scans through order-disorder phase transitions the rotation numbers increase monotonically with density, whereas the maximum Lyapunov exponent exhibits a pronounced maximum at the transition density [8,9]. The rotation numbers are also largest for indices belonging to the smallest exponents believed to be associated with the stability of collective modes in a fluid. We therefore speculate that the rotation spectra may prove useful for establishing a link between the linearized dynamics in tangent space and more traditional descriptions of systems in terms of (collective) modes. Examples for rotation

spectra are given in Sec. IV. Related numbers have been defined by Ruelle [21] and applied to two-dimensional maps by Lambert *et al.* [22].

It is instructive to view the dynamics of the δ vectors not only in the whole phase space but also in certain qualitatively different subspaces associated with special degrees of freedom. Since the phase space is a product of the center-of-mass configuration space Q, of the respective momentum space P, of the angular orientation space Ω for the molecular axes, and of the associated angular momentum space P_Ω, also the tangent space is decomposed into respective subspaces TQ, TP, $T\Omega$, and TP_Ω. We consider projections of the δ_l vectors onto $TX \in \{TQ, TP, T\Omega, TP_\Omega\}$:

$$\delta_{X,l} = \mathcal{P}(TX)\ \delta_l. \tag{14}$$

The projection operator $\mathcal{P}(TX)$ may be represented as a diagonal matrix with elements $\mathcal{P}_{\alpha\alpha}(TX)$ equal to unity if the α axis of δ_l belongs to TX and zero otherwise. We compute the time-averaged squared lengths of these projected vectors

$$\delta_{X,l}^2 = \langle \delta_{X,l} \cdot \delta_{X,l} \rangle \tag{15}$$

and refer to them as "mean-squared X components" of δ_l. Of course, for each l they add up to unity if summed over TX. They are a measure for the probability of a vector δ_l of pointing into the direction of tangent space belonging to the subspace TX. They turn out to be very helpful for the interpretation of our results. A related quantity $\cos^2\alpha^{(X)} \equiv \delta_{X,1}^2$ has been discussed recently by D'Alessandro and Tenenbaum [23], who refer to $\alpha^{(X)}$ as a coherence angle. It represents an effective angle between the subspace TX and the maximum-expansion subspace.

We have mentioned already that the constrained orthonormal-vector method of Eqs. (10)–(12) is conceptually very useful. However, any numerical solution of these equations involves quite extensive vector-matrix operations. Since the tangent vectors $\delta_l(t)$ obtained in this way are identical to the vectors generated by the classical method with continuous reorthonormalization, Eqs. (10)–(12) do not offer an improvement from a numerical point of view. For our numerical work we have therefore used the classical method of Benettin in combination with Gram-Schmidt reorthonormalization after every time step. To avoid the algebraic complexity we employed a finite-difference variant of the classical algorithm: The tangent vectors in (5) and (6) were approximated by finite offset vectors between two phase-space trajectories corresponding to a finite $s = 0.0001$. As many sets of the original motion equations (4) as the required number of Lyapunov exponents were integrated for the determination of the satellite trajectories and Gram-Schmidt reorthonormalization was carried out after every time step. A fourth-order Runge-Kutta algorithm with a reduced time step $\Delta t = 0.001$ was used for the integration. Every few time steps the molecular bonds were rescaled to their precise length to compensate for numerical inaccuracies. In all runs the trajectories were followed for at least 400 time units.

TABLE I. Simulation results for a density $n^* = 0.4$. d is the molecular bond length and is given in units of σ. n^d, the anisotropy-dependent density, is defined in the text. The maximum Lyapunov exponent λ_1 and the Kolmogorov entropy h_K are given in units of $(\epsilon/m\sigma^2)^{1/2}$.

d	n^d	λ_1	n_K
0.2	0.48	4.11	111.0
0.33	0.532	3.74	114.6
0.5	0.6	3.57	117.2
0.66	0.664	3.59	120.0
1.0	0.8	3.47	111.7

IV. RESULTS

The reduced molecular number density $n^* = N\sigma^2/V$ was chosen large enough to ensure sufficient coupling between translational and rotational degrees of freedom. Two series of simulation runs with n^* equal to 0.4 and 0.5 were performed. For a given n^* the molecular shape was varied by considering systems with different molecular bond length d. The anisotropy parameter d/σ was varied between 0.2 and 1.0 and the corresponding variation of the Lyapunov spectrum was determined. Since n^* does not account for the molecular anisotropy, we characterize our model systems also by an anisotropy-dependent density parameter $n^d = N\sigma(\sigma+d)/V$, which is, roughly speaking, the ratio of the occupied volume to the total. n^d becomes equal to n^* for isotropic particles. Some of our results for the maximum Lyapunov exponent λ_1 and for the Kolmogorov entropy h_k are summarized in Table I for $n^* = 0.4$ and in Table II for $n^* = 0.5$. Here the Kolmogorov entropy $h_K = \sum_{l=1}^{L/2}\lambda_l$ is given by the sum of the non-negative exponents. For all these simulations the kinetic energy per molecule was equal to 2, 2/3 for each translational and rotational degree of freedom. We monitored this partition of the kinetic energy among the translational and rotational degrees of freedom throughout the simulation. We found that equipartition among these degrees of freedom holds to within 3% for the whole range of densities, bond lengths, and temperatures.

The very different n^d dependence of λ_1 from that of h_k already suggests that the Lyapunov spectrum is considerably affected by the bond length. This may be verified from Fig. 1, in which all spectra with identical $n^* = 0.4$ but different d are displayed, and from the analogous Fig. 2 for $n^* = 0.5$. Of course, each spectrum consists of discrete

TABLE II. Simulation results for a density $n^* = 0.5$. d is the molecular bond length and is given in units of σ. n^d, the anisotropy-dependent density, is defined in the text. The maximum Lyapunov exponent λ_1 and the Kolmogorov entropy h_K are given in units of $(\epsilon/m\sigma^2)^{1/2}$.

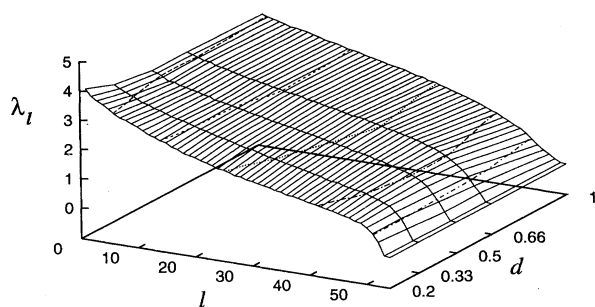| d	n^d	λ_1	h_k
0.2	0.6	5.08	134.1
0.33	0.665	4.56	135.9
0.5	0.75	4.36	133.3
0.66	0.83	4.02	115.0
1.0	1.0	3.16	65.2

FIG. 1. Lyapunov spectra for a planar fluid of 18 linear diatomic molecules at a reduced density $n^*=0.4$, for five different bond lengths d/σ equal to 0.2, 0.33, 0.5, 0.66, and 1.0. Only the positive branch (54 exponents, of which 3 vanish) is shown. The Lyapunov exponents are given in units of $(\epsilon/m\sigma^2)^{1/2}$. As usual, the index l merely numbers the exponents λ_l such that $l=1$ refers to the maximum exponent.

points only, which are located at the nodes of the connecting lines.

The index l along the abscissa merely numbers the exponents (or degrees of freedom), with $l=1$ for the maximum exponent, 51 for the smallest positive exponent, and 108 for the most negative exponent. For the construction of Figs. 1 and 2 only the positive branches (54 exponents) of the Lyapunov spectra were calculated and displayed. Due to the Smale-pairing symmetry for symplectic systems mentioned in the Introduction, the negative branch is obtained by reversing the sign of the positive branch. Six of the exponents must vanish due to the five constants of the motion—energy, center of mass, and linear momentum — and the fact that any perturbation in the direction of the phase flow adds another vanishing exponent. Vanishing exponents and their associated phase-space directions have indices $52 \leqslant l \leqslant 57$. However, for short bond lengths the exponent λ_{52} in Figs. 1 and 2 does not vanish exactly. This is an undesirable consequence of the periodic rescaling of the molecular bonds, but
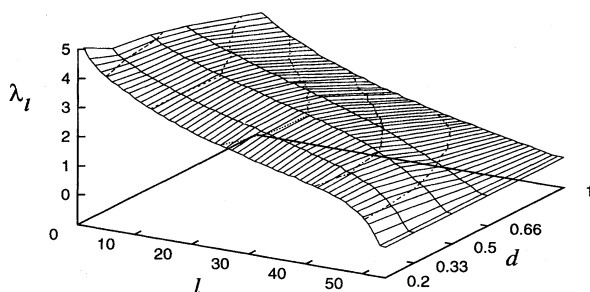
FIG. 2. Lyapunov spectra for a planar fluid of 18 linear diatomic molecules at a reduced density $n^*=0.5$, for five different bond lengths d/σ equal to 0.2, 0.33, 0.5, 0.66, and 1.0. Only the positive branch (54 exponents, of which 3 vanish) is shown. The Lyapunov exponents are given in units of $(\epsilon/m\sigma^2)^{1/2}$. As usual, the index l merely numbers the exponents λ_l such that $l=1$ refers to the maximum exponent.
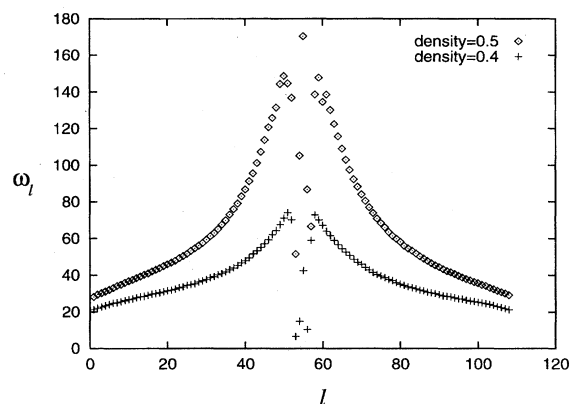

FIG. 3. Full rotation spectra (108 rotation numbers each) as defined in Sec. III, for a planar fluid of 18 linear diatomic molecules with a bond length $d/\sigma=1$, for the densities n^* equal to 0.4 (plus signs) and 0.5 (diamonds). The rotation numbers are given in units of $(\epsilon/m\sigma^2)^{1/2}$. The index l merely numbers the spectral points such that 1 corresponds to the maximum Lyapunov exponent, 108 to the minimum exponent.

does not affect the shape of the spectra.

For a few selected systems containing molecules with the longest $(d=\sigma)$ and the shortest bonds $(d=0.2\sigma)$ we computed also the full spectrum of 108 exponents together with the respective rotation numbers and mean-squared X components $\delta_{X,l}^2$. For the longest molecule $d=\sigma$, full rotation spectra are depicted in Fig. 3 for the densities $n^*=0.4$ and 0.5. Mean-squared X components are displayed in Fig. 4 for $n^*=0.5$, $d=\sigma$ and in Fig. 5 for $n^*=0.5$, $d=0.2\sigma$. These results will be discussed further in Sec. V.

In order to relate these findings to more traditional descriptions of the dynamics, we calculated also various time correlation functions referring to translational and rotational
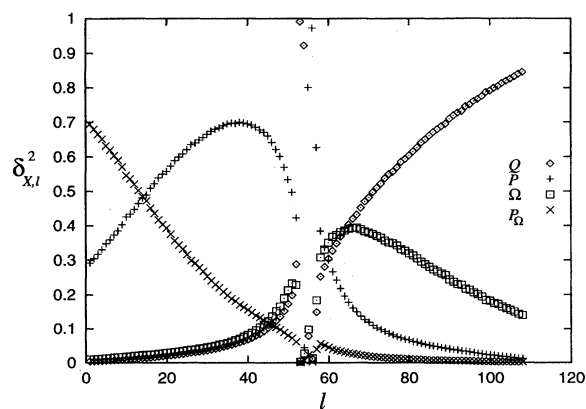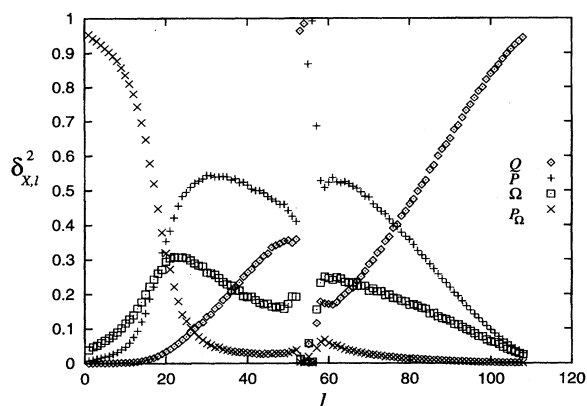

FIG. 4. Mean-squared X components $\delta_{X,l}^2$ as a function of the Lyapunov index l for a planar fluid of 18 linear diatomic molecules with a density $n^*=0.4$ and bond length $d/\sigma=1$. $l=1$ corresponds to the maximum Lyapunov exponent. The subspaces X are the center-of-mass configurational subspace Q (diamonds), the center-of-mass momentum subspace P (plus signs), the orientation-angle subspace Ω (squares), and the angular velocity subspace P_Ω (crosses).

FIG. 5. Mean-squared X components $\delta^2_{X,l}$ as a function of the Lyapunov index l for a planar fluid of 18 linear diatomic molecules with a density $n^* = 0.4$ and bond length $d/\sigma = 0.2$. $l = 1$ corresponds to the maximum Lyapunov exponent. The subspaces X are the center-of-mass configurational subspace Q (diamonds), the center-of-mass momentum subspace P (plus signs), the orientation-angle subspace Ω (squares), and the angular velocity subspace P_Ω (crosses).

motion of our model system. The normalized velocity auto-correlation functions for molecular center-of-mass motion, $C_{vv}(t) = \langle \mathbf{v}(t) \cdot \mathbf{v}(0) \rangle / \langle \mathbf{v}(0) \cdot \mathbf{v}(0) \rangle$, for the systems with the larger density $n^* = 0.5$ are shown in Fig. 6. Their time integral is related to the translational diffusion coefficient. Furthermore, the reorientational dynamics of linear molecules is usually discussed in terms of the correlation functions for the spherical harmonics of rank l of the angles specifying the orientation of the molecular axis. In three dimensions some of these correlation functions may be accessible by experiment, such as infrared absorption ($l = 1$), Raman scattering ($l = 2$), and neutron scattering (a weighted sum of $l > 0$ terms). For our planar model these rotational correlation functions are written as
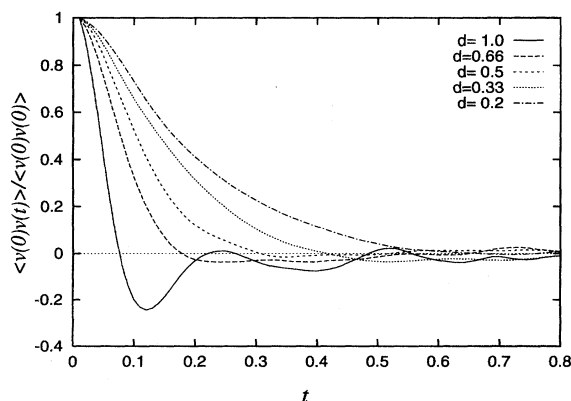

FIG. 6. Normalized velocity autocorrelation functions for a system of 18 linear diatomic molecules with a density $n^* = 0.5$ and different bond lengths d/σ varying between 0.2 and 1 as indicated. The time is given in units of $(m\sigma^2)^{1/2}$.
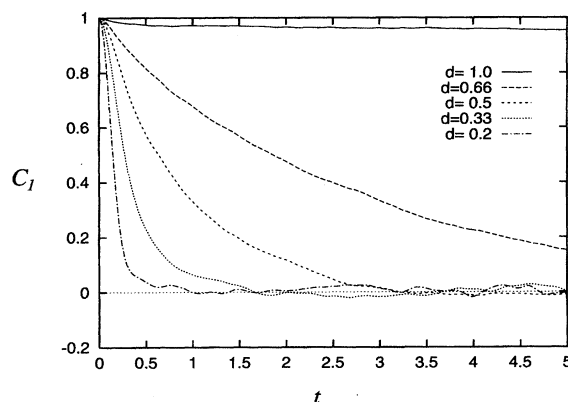

FIG. 7. Orientational correlation functions $C_1(t) = \langle P_1(\cos\Theta(t)) \rangle$ for a system of 18 linear diatomic molecules with a density $n^* = 0.5$ and different bond lengths d/σ varying between 0.2 and 1 as indicated. The time is given in units of $(m\sigma^2)^{1/2}$.

$$C_l(t) = \langle P_l(\cos[\Theta(t)]) \rangle, \tag{16}$$

where $\Theta(t) = \eta(t) - \eta(0)$ is the angle the axis of a molecule reorients during the time t and P_l denotes a Legendre polynomial of rank l. In Fig. 7 the functions $C_1(t) = \langle \cos[\Theta(t)] \rangle$ are depicted for the case $n^* = 0.5$ and the whole range of bond lengths. Similar results have been obtained also for C_2, but are not shown here.

V. DISCUSSION

The computation of L Lyapunov exponents requires the simultaneous integration of $L(L+1)$ first-order differential equations. Thus the number of molecules of a system accessible to present-day computation is much smaller than one is used to for traditional simulations of dynamical properties such as correlation functions or transport coefficients. For that reason our system consists of only $N = 18$ two-center molecules in a plane and the simulation box has a typical side length of 6σ (for $n^* = 0.5$). For such small systems it is difficult to distinguish between fluid and solid phases, although already systems of only two disks exhibit a first-order phase transition [24]. Nevertheless, we shall use these expressions to convey the general idea.

Before entering the discussion we stress again that six of the Lyapunov exponents vanish for reasons given above. They are located in the middle of the spectrum $52 \leq l \leq 57$ and the associated phase-space directions belong to the central manifold. Since Gram-Schmidt reorthonormalization has no ordering effect on the directions of their δ_l vectors, the respective rotation numbers in Fig. 3 and the squared X components in Figs. 4 and 5 have no meaning for $52 \leq l \leq 57$. We have nevertheless included these points in the figures to draw attention to this peculiarity.

An inspection of the center-of-mass velocity autocorrelation functions in Fig. 6 reveals that backscattering, typical for a dense fluid or solid, occurs only for the largest bond length. For this system C_1 in Fig. 7 does not decay and the orientation of the molecules persists for a long time. We conclude that this state is a solid, whereas all other systems

are fluids. This is also reflected in the shape of the Lyapunov spectra, which for $d = 1.0$ and $n^* = 0.5$ in Fig. 2 is very similar to that of a two-dimensional solid formed with isotropic particles [2]. Also the empirical power law

$$\lambda_l / \lambda_1 = \left[\left(\frac{L}{2} - 2 - l \right) \Big/ \left(\frac{L}{2} - 3 \right) \right]^\beta \qquad (17)$$

for $1 \leq l \leq L/2 - 2$ works reasonably well with an exponent $\beta = 3/2$ [2]. λ_1 is the maximum exponent. As expected, the shape of all other spectra conforms closely to that of atomic fluids [2], but a representation in terms of such a power law is not appropriate.

The maximum Lyapunov exponent λ_1 describes the time evolution of the small perturbation, which grows fastest in phase space. It is a local quantity in the sense that it depends basically on the fastest dynamical events taking place in the system, namely, collisions, for which the velocities and angular velocities change sign. It is a reasonable assumption that the fastest phase-space growth takes place in the linear and angular momentum subspaces. The mean-squared X components $\delta^2_{X,l}$ introduced in Sec. III support this view. Simulations for atomic systems have revealed that δ_1 is located almost fully in the momentum related subspace TP of tangent space. For the linear molecules studied here the angular-momentum related subspace TP_Ω of tangent space turns out to be the most important. Figure 4 shows that on the average 69% of the squared length of δ_1 for the elongated molecular case ($d = 1$) is contributed by TP_Ω. This number even rises to 96% for the more freely rotating case in Fig. 5 ($d = 0.2$). We conclude that the main reason for the instability of the phase-space trajectory is due to the anisotropy of the pair potential and it is mostly accumulated in the angular-momentum subspace.

The situation changes completely when we consider δ_l vectors for $l > 1$ pointing into less-violently expanding or even compressing phase-space directions. Figures 4 and 5 reveal that the linear-momentum subspace becomes dominant for, say, $20 \leq l \leq 51$, still associated with positive exponents. In this range the prominent contributions to the Lyapunov spectra comes from translational modes, which one is tempted to associate with generalized "hydrodynamical" modes with small but finite wave vectors. An approximate representation of these translation-dominated exponents in terms of the power law (17) leads to exponents $\beta < 1$ similar to that of atomic fluids [2]. It follows that the positive curvature of the Lyapunov spectra in Figs. 1 and 2 for the most positive exponents (small l) is essentially due to contributions from rotational degrees of freedom, which make themselves felt more distinctly for small d associated also with small moments of inertia.

It is interesting to note that the stable phase-space directions corresponding to the negative Lyapunov exponents are dominated by the configurational subspace Q and, to a lesser extent, by the orientation-angle subspace Ω (Fig. 4). The significance of this is not clear to us.

That the maximum exponents of Figs. 1 and 2 increase with density n^* for fixed d and constant temperature is easily explained by the increase of the collision frequency. The relative maximum exhibited by the positive exponents of Fig. 2 as a function of the bond length is less obvious, since

an increase of d for constant n^* also increases the collision rate. This maximum is a consequence of the phase transition eventually leading to a solid for $d = 1$. In the less-dense case of Fig. 1 this maximum is expected to occur for bond lengths slightly larger than σ. Similar maxima for λ_1 as a function of density have been observed previously for fluid-to-solid phase transitions in atomic-particle systems [8].

The rotation numbers measure the average speed of rotation of the δ_l vectors in phase space. From simple arguments involving the time-reversal invariance of the original motion equations (4) and of their linearized version (7) we expect that the rotation spectra for symplectic systems are symmetric such that $\omega_l = \omega_{L+1-l}$. This symmetry was observed for atomic systems [8] and is also apparent in Fig. 3 for the linear-molecule case with $d = 1$. The theoretical significance of these numbers is still controversial. Also the N dependence of these numbers needs to be investigated.

The Kolmogorov entropy h_K is a global measure of the rate with which information is generated by the dynamics and hence of the disorder in such an equilibrium system. Our numerical results tabulated in Tables I and II confirm the general picture outlined above. For $n^* = 0.5$ this parameter varies only very little with the molecular anisotropy as long as the system remains fluid (Table II). It starts to decrease, when the phase transition is approached, and becomes significantly smaller for the solid. This transition takes place near an anisotropy-dependent density $n^d = 0.8$. For the lower density $n^* = 0.4$ a similar transition occurs near $n^d = 0.8$, although d must be increased beyond 1 for a solid to be observed. This "transition density" agrees with the phase-transition density of an isotropic-particle system, at which the maximum Lyapunov exponent reaches a maximum [8,9].

VI. CONCLUSION

This work is an attempt to survey the (in)stability properties of phase-space trajectories for systems of anisotropic molecules. A detailed analysis of the Lyapunov spectra as a function of density and molecular anisotropy makes it possible to distinguish, at least qualitatively, the contributions from the center-of-mass motion and of molecular reorientation. We find that the major contributions to the instability of the phase-space trajectory come from the rotational degrees of freedom and, in particular, from the angular-momentum variables. Translational center-of-mass motion is much less destabilizing. Although, for practical reasons, the systems contain only a few molecules, the influence of the fluid-solid phase transition on the Lyapunov instability and the Kolmogorov entropy is clearly seen. One might speculate that an even more detailed analysis of the dynamics of the tangent vectors in the respective subspaces spanned by the center-of-mass coordinates, the corresponding momenta, the orientation angles, and the angular velocities may lead to an interpretation in terms of collective modes in many-body systems. We are still far away from this goal, but it is hoped that recent progress in the methodology of computing Lyapunov spectra for systems of hard core particles [25,26,9] will also be useful for the understanding of anisotropic molecular systems.

ACKNOWLEDGMENTS

[1] H. A. Posch and W. G. Hoover, Phys. Rev. A **38**, 473 (1988).

[2] H. A. Posch and W. G. Hoover, Phys. Rev. A **39**, 2175 (1989).

[3] D. J. Evans, E. G. D. Cohen, and G. P. Morriss, Phys. Rev. A **42**, 5990 (1990).

[4] S. Sarman, D. J. Evans, and G. P. Morriss, Phys. Rev. A **45**, 2233 (1992).

[5] V. I. Arnold, *Mathematical Methods of Classical Mechanics* (Springer, New York, 1983).

[6] H. A. Posch and W. G. Hoover, Phys. Rev. E **49**, 1913 (1994).

[7] W. G. Hoover, C. G. Hoover, and H. A. Posch, Phys. Rev. A **41**, 2999 (1990).

[8] H. A. Posch, W. G. Hoover, and B. L. Holian, Ber. Bunsenges. Phys. Chem. **94**, 250 (1990).

[9] Ch. Dellago, H. A. Posch, and W. G. Hoover, Phys. Rev. E **53**, 1485 (1996).

[10] H. A. Posch and S. Toxvaerd (unpublished).

[11] D. J. Evans and G. P. Morriss, *Statistical Mechanics of Nonequilibrium Liquids* (Academic, London, 1990).

[12] W. G. Hoover and H. A. Posch, Phys. Lett. A **113**, 82 (1985).

[13] V. I. Oseledec, Moscow Math. Soc. **19**, 197 (1968).

[14] J. P. Eckmann and D. Ruelle, Rev. Mod. Phys. **57**, 617 (1985).

[15] G. Benettin, L. Galgani, A. Giorgilli, and J. M. Strelcyn, C. R. Acad. Sci. (Paris) **286**, 431 (1978).

[16] G. Benettin, L. Galgani, A. Giorgilli, and J. M. Strelcyn, Meccanica **15**, 9 (1980).

[17] I. Shimada and T. Nagashima, Prog. Theor. Phys. (Jpn.) **61**, 1605 (1979).

[18] A. Wolf, J. B. Swift, H. L. Swinney, and J. A. Vastano, Physica D **16**, 285 (1984).

[19] I. Goldhirsch, P. L. Sulem, and S. A. Orszag, Physica D **27**, 311 (1987).

[20] W. E. Wiesel, Phys. Rev. E **47**, 3686 (1993)

[21] D. Ruelle, Ann. Inst. Poincaré **42**, 109 (1985).

[22] A. Lambert, R. Lima, and R. Vilela Mendes, Physica D **34**, 366 (1989).

[23] M. D'Alessandro and A. Tenenbaum, Phys. Rev. E **52**, R2141 (1995).

[24] B. J. Alder, W. G. Hoover, and T. E. Wainwright, Phys. Rev. Lett. **11**, 241 (1963).

[25] Ch. Dellago and H. A. Posch, Phys. Rev. E **52**, 2401 (1995).

[26] Ch. Dellago, L. Glatz, and H. A. Posch, Phys. Rev. E **52**, 4817 (1995).